IOP Conf. Series: Materials Science and Engineering **1327** (2025) 012109 doi:10.1088/1757-899X/1327/1/012109

Cryogenic options for future accelerators: case study for the Muon Collider ring†

P. Borges de Sousa[1], B. Naydenov[1], L. Delprat[1], T. Koettig[1], and R. van Weelderen[1]

[1]CERN, Esplanade des Particules 1, 1211 Geneva 23, Switzerland

E-mail: pat.borges.sousa@cern.ch

Abstract. Future, multi-km particle accelerator projects will be under heavy scrutiny to be energetically sustainable. Compared to previous accelerators, these machines must sustain increasingly high beam-induced, static, and dynamic heat loads per meter length. These features make the cryogenic infrastructure, required for superconducting magnet operation, a major cost and energy consumption driver. The choice of a general cooling scheme and associated superconductor temperature operating window that optimizes both is essential. With cost-effectiveness, simplicity, and a reduction in reliance on cryogen availability and market volatility in mind, the virtues of having magnets that would incorporate conduction cooling, thus avoiding full immersion in helium, and that operate at increasingly higher temperatures, are examined. This study presents an overview of cooling options for collider-type magnets, discussed in the context of the collider ring of the Muon Collider. The main drivers when choosing a cryogenic system for future accelerators are identified and guidelines for magnet thermal design are established. A conceptual study of cooling schemes that fulfil these guidelines is presented and compared to present and past choices for accelerator magnet cooling.

1 Introduction

The update of the European Strategy for Particle Physics has recommended for an international design study for a muon collider to be integrated in the European Roadmap for Accelerator R&D. This led to the creation of the International Muon Collider Collaboration (IMCC) [1], that builds on previous studies to evaluate the feasibility of both a 3 TeV and a 10 TeV centre-of-mass energy collider. An overview of the Muon Collider complex can be found in [2].

While a cryogenic infrastructure will be required throughout the accelerator complex for a large variety of both magnets and cavities, the collider ring will consist exclusively of superconducting magnets operating in an environment with unprecedented heat loads due to muon decay [3], making the collider the most demanding part of the complex from a cryogenic power consumption perspective. For this reason, the study presented here has been directed towards the collider magnets.

At this early stage in the conceptual design, where the magnets start to take shape, the operating temperature levels of system components such as cold mass, beam screen/absorber, and thermal shields need to be defined. This will depend not only on the choice of conductor, one of the main drivers, but also on the need for reduced complexity, on the limits of local heat extraction, and on the overall cost of cooling. In turn, local heat extraction strategies and electrical power consumption depend heavily on the heat loads that need to be cooled away and at which temperature. This study aims to define the range of expected heat loads on the collider magnets and to provide an estimate of the resulting cooling effort for each option.

†on behalf of the IMCC.

2 General layout of the collider magnets

The collider ring will be composed mostly of combined function magnets, which integrate multipolar components into the arc dipoles. This allows for a reduction of field-free straight sections and for mitigation of the significant neutrino flux. The magnets need to provide a high dipolar magnetic field to minimize the collider ring circumference and maximise luminosity; presently the study considers, for a 10 TeV collider, arc magnets that generate a steady-state magnetic field of up to 16 T in a 150 mm aperture [4]. The rather large aperture is necessary to accommodate the appropriate aperture for the beam, a thick particle radiation absorber, vacuum insulation, the magnet cold bore/beam pipe, and support and cooling structures. The absorber is essential to shield the magnet coils from radiation generated by muon decay products (roughly 1/3 of beam energy, about 500 $\mathrm{W\,m^{-1}}$ [5]), and to intercept the heat load due to the secondary particles generated by the muon decay at a temperature higher than that of the cold mass. This sizeable heat load requires the absorber to be operated at the highest possible temperature to reduce cryogenic power consumption, while maintaining appropriate thermal decoupling between the absorber and the coil in a narrow annular space within the magnet aperture. Still, a portion of this heat load will penetrate the absorber, the fraction of which depends on the absorber's thickness and ranges from 4 $\mathrm{W\,m^{-1}}$ for a 40 mm-thick absorber to 18 $\mathrm{W\,m^{-1}}$ for a 20 mm-thick one.

Figure 1 outlines a tentative radial build for the collider ring magnets. The beam aperture (5σ) has a radius of 23.5 mm, surrounded by a tungsten absorber between 20 mm and 40 mm (30 mm shown in Figure 1). The inner surface of the tungsten absorber is coated with a 0.01 mm copper layer that acts as a beam screen. The absorber and the cold bore of the magnet (beam pipe) are separated by a thermal shield (labelled as heat intercept in Figure 1), with 5 mm clearance on each side. Finally there is the beam pipe, which supports the magnet coils and creates the beam vacuum-magnet separation.

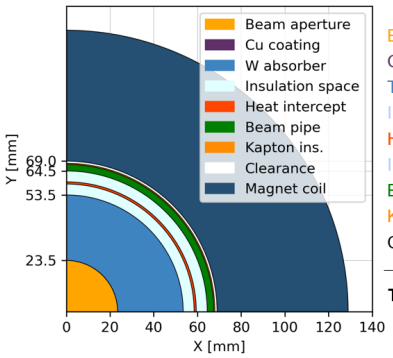

	Δr
Beam aperture (5σ)	23.49 mm
Cu layer beam screen	0.01 mm
Tungsten absorber	20-40 mm
Insulation space	5 mm
Heat intercept	1 mm
Insulation space	5 mm
Beam pipe	3 mm
Kapton insulation	0.5 mm
Clearance to coils	1 mm
Total magnet aperture	**118-158 mm (diameter)**

Figure 1: Tentative radial build for the collider ring magnets, highlighting the different space allocations inside the magnet aperture, shown here for an absorber thickness of 30 mm. Note that the coil thickness (shown in dark blue) is arbitrary and for illustration purposes only.

The goal of the thermodynamic design for the collider magnets is to intercept the largest possible fraction of heat loads at the highest possible temperatures, while operating the magnet itself at the highest practical temperature. To this end, the sources and dependencies of heat load to each component (*i.e.* temperature level) need to be identified and estimated. Figure 2 schematises the sources of steady-state heat loads in the different parts of the magnet system for the different temperature levels of the cryostat, as well as their dependence on temperature and absorber dimensions. The absorber intercepts the bulk of the beam-induced heat loads, which depend on beam parameters but are mostly temperature- and thickness-independent. Image currents, synchrotron radiation, and beam-gas scattering are also present, however their contribution to the total heat load ($\mathrm{O}(1\,\mathrm{W\,m^{-1}})$) is negligible when compared to muon decay and has therefore not been considered. At the outer thermal shield level, the heat loads are due mainly to radiation from the room temperature vacuum vessel, and to solid conduction via the supporting posts of the cold mass. The inner thermal shield ("heat intercept" in Figure 1) intercepts incoming thermal radiation from the absorber. The current lead intercepts, as well as the contribution from the resistive splices in the magnets, are yet to be defined.

3 Heat load estimation

The estimation of heat loads at each temperature level can be carried out for a set of temperatures for each part of the system. We considered cold mass temperatures of 2 K, 4.5 K, 10 K and 20 K for our

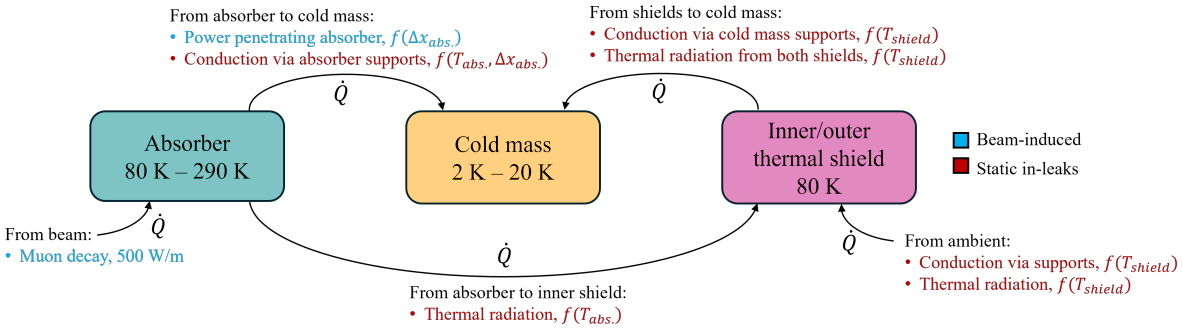

Figure 2: Sources of steady-state heat load in the magnet system for a 10 TeV muon collider ring. The boxes represent the three temperature levels in the system along with the range of temperatures considered in this study, while the contributions from each component to the others are represented by arrows, which are divided into beam-induced and static heat in-leaks.

study: 2 K is included for comparison with current machines like the LHC; 4.5 K could be the operating temperature for a design using Nb_3Sn magnets; and 10 K and 20 K are potential temperature ranges if the magnets are built using High Temperature Superconductor (HTS) technology. Note that these values are considered for a simplified estimation of heat loads; in reality, the magnets will be subjected to a temperature *range* and not an isothermal environment. Whereas one can assume quasi-isothermal cooling along an arc when considering helium cooling in saturated conditions at 4.5 K, operation in supercritical conditions at around the same temperature implies an inherent gradient along the magnet (and arc) length in the order of 1 K. If cooling at 10 K or 20 K using helium gas, the temperature gradient would be larger, in the order of tens of K.

The contribution by thermal radiation from the outer thermal shield was calculated assuming 30 layers of multilayer insulation (MLI) on the shield and 10 layers on the cold mass. The thermal radiation to the cold mass from the inner shield between absorber and beam pipe was calculated assuming mechanically polished copper (for the shield) and stainless steel (for the beam pipe). Heat load via the supporting posts of the cold mass was scaled from LHC supports [6]. We consider that the absorber is supported by the beam pipe via rolling structures with low thermal conductivity, similar to the HL-LHC beam screen [7] or the transfer units for the PUMA experiment [8]. Due to the considerable weight of the tungsten absorber (around 140 kg m^{-1} for 30 mm thickness), the heat load to the beam pipe was estimated by scaling the results obtained for the PUMA transfer units, while assuming no intermediate thermalisation to the inner shield. Finally, at the level of the cold mass, the beam-induced radiation penetrating the absorber depends only on the absorber thickness [5]; we considered 30 mm for this study, since it keeps the magnet aperture below 150 mm while keeping the beam-induced load below 10 W m^{-1} [9].

The heat load due to muon decay for a 10 TeV machine is ≈500 W m^{-1}. This is an unprecedented heat load in a superconducting machine (for comparison, the heat load generated by electron cloud effects in the arc magnets in HL-LHC is a few W m^{-1} [10]) and should be extracted at the highest possible temperature: for this study, we consider an operating range for the absorber between 80 K and 290 K.

The shields that intercept thermal radiation from both the vacuum vessel of the cryostat (outer shield) and from the absorber (inner shield) were fixed at 80 K. Although the temperature level can be the object of an optimization exercise, the heat load extracted at this temperature level is not the determining factor in the budget for power consumption, as will be shown in this study.

Figure 3 shows the calculated heat load deposited at the cold mass for four nominal temperatures: 2 K, 4.5 K, 10 K and 20 K. The heat loads at the thermal shield level vary between 4 W m^{-1} and 11 W m^{-1} depending on absorber temperature, while the absorber itself has a constant heat load of 500 W m^{-1}.

The heat load from muon decay that penetrates a 30 mm absorber is by far the largest contribution at 8 W m^{-1}, followed by the absorber supports. The contribution from thermal radiation from either the inner shield inside the beam pipe or the outer shield is minimal. While the overall heat load to the cold mass depends on the absorber temperature (mostly due to the influence it has on heat load by conduction via the supports), its dependence on the cold mass temperature itself is negligible, as can be observed by comparing the four plots in Figure 3. The effort to extract this heat load will however depend significantly on the chosen cold mass temperature.

A first iteration of this estimation exercise was carried out for a configuration where there was no

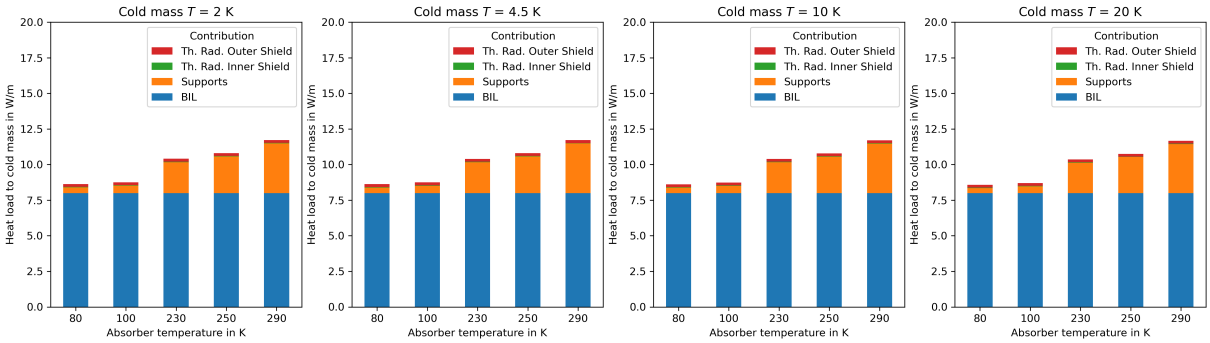

Figure 3: Heat load deposited on the cold mass in $\mathrm{W\,m^{-1}}$, as a function of absorber temperature, for an absorber thickness of 30 mm, for nominal magnet operating temperatures of 2 K, 4.5 K, 10 K and 20 K. The thermal shields (inner shield between absorber and coil, and outer shield) are assumed to be at 80 K. In the legend, "BIL" stands for "beam-induced losses".

inner thermal shield, *i.e.*, the absorber and the cold mass were in direct line of sight: as a result, at absorber temperatures higher than 200 K, the radiation heat load from absorber to cold mass exceeded that of the beam-induced losses for certain absorber thicknesses. This was deemed unacceptable and it was decided to add an inner thermal shield between absorber and cold mass to the baseline radial build. This allows for a two-fold advantage: the absorber heat loads can be extracted at higher temperatures while keeping the heat load to the cold mass low and less dependent on the absorber temperature.

4 Cryogenic power consumption

From the 2021 Snowmass report, the electrical power to operate the Muon Collider is estimated at 300 MW [11]. A proposed target of 10% of that power (30 MW) is taken for the cryogenic operation of the whole complex, with 25 MW allocated to the collider ring. This means that for a 10 TeV, 10 km ring, the electrical power consumption of the cryogenic infrastructure should remain below $2.5\,\mathrm{kW\,m^{-1}}$.

A semi-realistic estimate of overall power consumption for each temperature level can be carried out using the real inverse coefficient of performance ($\mathrm{COP^{-1}}$) of existing cryogenic insfrastructures (LHC cryoplant data [12, 13], LN_2 plants [14]). Figure 4 shows the total power consumption at refrigerator interface for different pairs of absorber and cold mass temperatures, while considering the thermal shields at 80 K. Note that the estimated power consumption does not include distribution effort, which will increase the overall consumption and is dependent on the cooling scheme and choice of fluid.

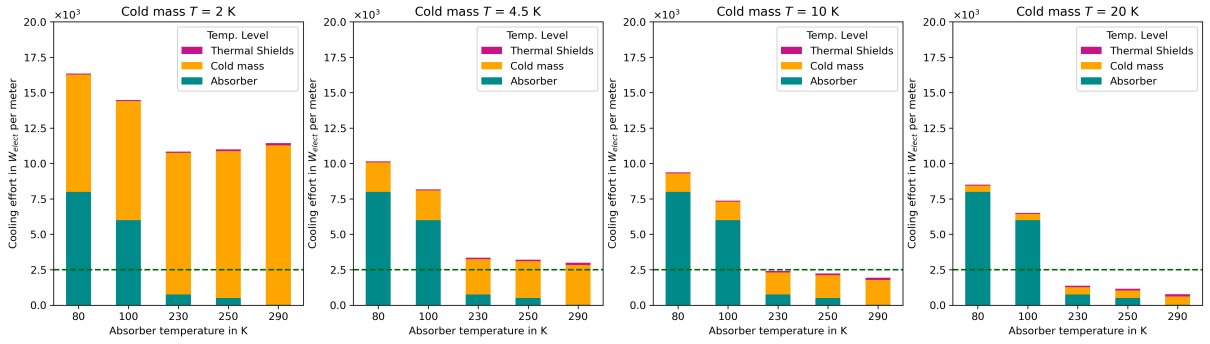

Figure 4: Power consumption at refrigerator interface, in $\mathrm{W\,m^{-1}}$, as a function of absorber temperature, for an absorber thickness of 30 mm, nominal magnet operating temperatures of 2 K, 4.5 K, 10 K and 20 K. The thermal shields are fixed at 80 K. The different components of the bars reflect the temperature level at which the cooling effort is calculated. The green dashed line represents the maximum electrical power consumption allocated for the collider ring.

To stay within the set targets for power consumption for the collider ring, shown by a horizontal dashed line in Figure 4, a few combinations of cold mass/absorber temperature are immediately excluded.

From this analysis, the absorber should be cooled to a temperature higher than $\approx 200\,\mathrm{K}$, while 2 K cold mass operation is prohibitively costly and can be excluded based on power consumption alone. A collider ring with magnets operating at 4.5 K (*i.e.* using Nb_3Sn) could be carefully designed to be close to the power consumption budget, and remains a valid option for magnet design; designs at 10 K and 20 K remain more energetically favourable and allow for more comfortable margins for distribution losses and contingency for transients. Note that the larger the "cold mass" component in Figure 4, the more challenging the coil/cold mass design, as local heat extraction from the solid components to the cooling source becomes the bottleneck.

5 Cooling options: considerations

The overall definition of a cooling scheme for the collider is an iterative process. On one hand, looking to minimise cost and maximise availability, one should consider as few cryoplants as possible; this will however increase the length of each sector to be cooled, which has implications on the maximum available cooling capacity of an individual cryoplant and on the available pressure drop for the sector. The sizing of the cryogenic system, namely the size and integration of the distribution line, will also depend on the allowed temperature gradient along a sector for the magnet string, which in turn depends on the choice of conductor (HTS magnets can in principle tolerate a higher ΔT than Nb_3Sn).

Operation of a muon collider ring at 2 K has been excluded in the previous section on the basis of power consumption. There are however other reasons to move away from bath cooling in He and in He II in particular. He II cooling provides nearly-isothermal temperatures and a large enthalpy reservoir, but relies on cold compressors which are complex to operate and have limitations in terms of suction pressure and mass flow rates. Also, operation below 4.5 K requires sub-atmospheric conditions in the pumping lines along considerable distances, adding technical challenges to the distribution line.

Due to the amount of helium required in the cryostats, management of helium inventory and safety related aspects become rather complex in case of disruptions such as a magnet quench; additionally, for He II, the large enthalpy difference of the transition from He I to He II increases operational downtime, reducing the accelerator's availability. The authors consider that cryogenic systems for future accelerators shall have in mind cooling schemes that are based on reduced amounts of cryogenic fluid, namely by switching from a bath-type configuration to forced flow along cooling channels embedded into the cold mass, for example.

For a cold mass operating at around 4.5 K, cooling could be achieved using either two-phase helium at 4.5 K or using supercritical helium between 4.5 K and 5 K at 0.3 MPa, both in a forced flow configuration inside cooling channels. In either case, provisions need to be made for coping with transient heat loads, such as a quench or current ramping losses, as a system with reduced helium content lacks the enthalpy reservoir provided by a bath. Options using HTS (operation at or above 10 K) involve using helium gas at high pressure or, for temperatures at or above 21 K, two-phase hydrogen; in either case, the same strategy of forced flow in small channels is envisaged. While using helium gas at high pressure is well established, the heat transfer and available enthalpy difference are rather poor above 10 K, requiring large temperature differences along a magnet sector and radially within the cold mass. Hydrogen, on the other hand, has a high available enthalpy (at 21 K, 12 times higher by volume than helium at 4.5 K), necessitating comparably smaller mass flow rates delivered to the cold masses. It is, unlike helium, an abundant resource, and investments from other fields in industry could bridge the current shortcomings in cost, storage, and safety assessments. Its exploration as a viable technical coolant for future colliders has recently started [15].

Presently considered options for the absorber circuit include water ($T_{abs.} > 280\,\mathrm{K}$) and CO_2 ($250\,\mathrm{K} > T_{abs.} > 280\,\mathrm{K}$). CO_2 is commonly used in detector cooling, and presents a few key advantages. Cooling circuits can be designed operating at high pressure (6 MPa and over) which allow for cooling over long distances in small cooling channels with acceptable distribution losses, and the high available enthalpy reduces the overall amount of fluid. In addition, it is radiation hard, has a high heat transfer coefficient, and can be a safer alternative to water systems even at temperatures close to ambient, as it eliminates the risk of water leaks [16] or freezing (expanding) water inside the cooling channels.

6 Conclusions and outlook

Considering the various constraints imposed by the main drivers, which combine both sustainability and technical requirements, a few guidelines for magnet design and operation can be drafted from this preliminary study. The heat load deposited at the absorber level shall be lifted at or above 250 K. The heat load to the cold mass shall remain at or below $10\,\mathrm{W\,m^{-1}}$, which requires both an absorber of at least 30 mm and an inner thermal shield, and the cold mass shall be cooled at a base temperature of 4.5 K or

higher. The overall electrical power consumption of the cryogenic system for the collider magnets shall not exceed 2.5 kW m^{-1}. For the heat load to the coil to remain at or below 10 W m^{-1}, an inner thermal shield between the absorber and the coil is essential. Complementary to these guidelines, the design of a sustainable cryogenic infrastructure for the muon collider ring shall be based on forced flow along cooling channels (as opposed to immersion cooling) to reduce the overall amount of coolant in the system, which has availability, economical and safety advantages. R&D to explore the limits of two-phase flow and supercritical cooling in confined geometries is needed, especially for helium and potentially hydrogen, to validate this type of cooling at an accelerator scale.

So far, this preliminary study has focused on the steady-state heat loads. The transient loads, *e.g.* hysteresis losses due to magnet ramping, should however not be neglected in future studies as they might become the driving factor for sizing the cryogenic system for the collider. This is true for Nb_3Sn but especially for any magnet concept based on HTS, as the losses in this type of conductor can easily be 1-2 orders of magnitude higher than the currently achievable values for Nb_3Sn.

References

[1] D. Schulte. "The International Muon Collider Collaboration". In: *JACoW IPAC* 2021 (2021), pp. 3792–3795. DOI: 10.18429/JACoW-IPAC2021-THPAB017.

[2] The International Muon Collider Collaboration. URL: https://muoncollider.web.cern.ch/about-study.

[3] C. Accettura et al. "Towards a Muon Collider". In: *Eur. Phys. J. C* 83.9 (2023), p. 864. DOI: 10.1140/epjc/s10052-023-11889-x. arXiv: 2303.08533.

[4] S. Fabbri et al. "Magnets for a muon collider". In: *JACoW IPAC* 2023 (2023), WEPM062. DOI: 10.18429/JACoW-IPAC2023-WEPM062.

[5] D. Calzolari et al. "Radiation Load Studies for Superconducting Dipole Magnets in a 10 TeV Muon Collider". In: *JACoW IPAC* 2022 (2022), pp. 1671–1674. DOI: 10.18429/JACoW-IPAC2022-WEPOST001.

[6] M. Castoldi et al. *Thermal Performance of the Supporting System for the Large Hadron Collider (LHC) Superconducting Magnets*. Tech. rep. LHC-Project-Report-335. CERN, 1999.

[7] P. Borges de Sousa et al. "Parametric study on the thermal performance of beam screen samples of the High-Luminosity LHC upgrade". In: *IOP Conference Series: Materials Science and Engineering* 278.1 (2017), p. 012053. DOI: 10.1088/1757-899X/278/1/012053.

[8] J. Liberadzka. *The Thermal Conductivity of Ball Transfer Units under Compression Force for the PUMA Project*. Tech. rep. CERN, 2021. URL: https://edms.cern.ch/document/2443998/3.

[9] V. V. Kashikhin et al. "High-Field Combined-Function Magnets for a 1.5 x 1.5 TeV Muon Collider Storage Ring". In: *Conf. Proc. C* 1205201 (2012). Ed. by V. Suller, pp. 3587–3589.

[10] O. Aberle et al. *High-Luminosity Large Hadron Collider (HL-LHC): Technical design report*. CERN Yellow Reports: Monographs. CERN, 2020. DOI: 10.23731/CYRM-2020-0010.

[11] T. Roser et al. "On the feasibility of future colliders: report of the Snowmass'21 Implementation Task Force". In: *Journal of Instrumentation* 18.05 (May 2023), P05018. DOI: 10.1088/1748-0221/18/05/p05018.

[12] H. Gruehagen and U. Wagner. "Measured Performance of Four New 18 kW@4.5 K Helium Refrigerators for the LHC Cryogenic System". In: LHC-Project-Report-796 (2005).

[13] S. Claudet et al. "1.8 K Refrigeration Units for the LHC: Performance Assessment of Pre-series Units". In: LHC-Project-Report-797 (2005).

[14] C. Gondrand et al. *Air Liquide cryogenic solutions for HTS refrigeration*. Presented at the ICEC/ICMC 2014 conference. 2014. URL: https://indico.cern.ch/event/244641/contributions/1563442/.

[15] S. Prestemon. *US Magnet Development Program and synergies with FCC-hh*. Presented at the FCC week 2024. 2024. URL: https://indico.cern.ch/event/1298458/contributions/5977856/.

[16] B. Verlaat and A. P. Colijn. "CO2 Cooling Developments for HEP Detectors". In: *PoS* VERTEX 2009 (2010), p. 031. DOI: 10.22323/1.095.0031.